Eur. Phys. J. Spec. Top. (2023) 232:179–185
https://doi.org/10.1140/epjs/s11734-022-00685-5

THE EUROPEAN PHYSICAL JOURNAL
SPECIAL TOPICS

Regular Article

Continuous baseline update using recurrence quantification analysis for damage detection with guided ultrasonic waves

Björn Maack[1,a], Carsten Brandt[2], Michael Koerdt[1], Christoph Polle[1], and Axel Siegfried Herrmann[1]

[1] Faserinstitut Bremen e. V., Measurement Systems and Monitoring, Am Biologischen Garten 2, 28359 Bremen, Germany
[2] Private Researcher, Rüdesheimer Straße 13, 28199 Bremen, Germany

Received 29 June 2022 / Accepted 27 September 2022 / Published online 4 November 2022

Abstract For the safe operation of vehicles and full utilization of lightweight materials, assurance of structural integrity is a prerequisite at all times. Structural health monitoring with permanently installed transducers offers a great advantage for primary load-bearing structures of all means of transportation and other safety-relevant components such as hydrogen tanks: allowing damage detection during operation. One means to detect internal defects is the method of guided ultrasonic waves (GUWs), which can be generated and recorded by piezoelectric transducers. GUWs propagate along the elongated dimension of a structure, and a transducer network can completely cover and monitor structures. Defects can alter the signal along affected paths and allow for their detection. However, a challenge and obstacle for the application of such a testing technique in the service of means of transportation is the large influence of temperatures. These influences are difficult to distinguish from the effect of defects. One approach to overcome this difficulty is the "continuous baseline update". Recurrence quantification analysis is tested and compared to established features as a new approach to "continuous baseline update" in this paper. Publicly available GUW data (http://www.openguidedwaves.de/) recorded under varying temperature conditions have been used to show how the methods perform. They reliably separate temperature and damage effects, while the recurrence quantification analysis yields the best results.

1 Introduction

Guided ultrasonic waves (GUWs) are used for structural health monitoring (SHM) in plate-like structures as the waves are sensitive to damage causing a change in wave propagation. SHM data of GUW propagation are recorded by transducers that are permanently bonded to the structure to be monitored. However, GUWs and the SHM system are also sensitive to variations in environmental and operational conditions (EOC) that do not relate to damage [1].

Thus, a change in the data can indicate the occurrence of damage when the measurement is compared with a reference signal, the so-called baseline, which was recorded on the healthy structure under the same EOC. Methods are needed to overcome the effects of non-damage-related changes in the recorded data, causing differences in the baseline. In [2] a review of such methods is provided and discussed. Time-domain subtraction methods have been developed, not using a prestored fixed baseline or baseline set but instantaneously measured GUW signals [3], instantaneous baseline measurements [4], relative baselines [5], and updating baselines [6–8], for damage detection to overcome challenges in a dynamic environment. The method described in [6] collects the baselines during service life and the baseline set grows continuously. The methods proposed in [7] and [8] are based on a continuously updated baseline. In [7] the "continuous baseline update" is used for fatigue crack monitoring, in [8] for damage detection on a carbon fiber reinforced plastic (CFRP) plate under variable temperature conditions. Different feature extraction methods are applied to evaluate signal changes for damage detection. Commonly used simple methods are subtraction of waveforms or comparison of amplitudes (maximum amplitude method). Other approaches are based on data reduction like principal component analysis to compute the eigenvalue of a signal, i.e., one value characterizes a recorded senor signal. Computation can be executed via eigenvalue decomposition or singular

Guest editors: Norbert Marwan, Charles Webber Jr., Andrzej Rysak.

[a] e-mail: maack@faserinstitut.de (corresponding author)

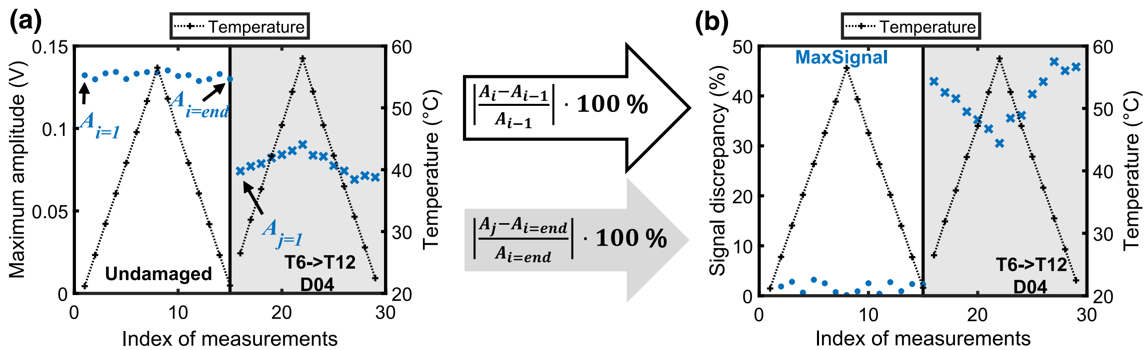

Fig. 1 Determination of the signal discrepancy (SD) according to the continuous baseline update approach using the example of MaxSignal (maximum amplitude values as extracted feature); data used from [8] and explained in Fig. 2. **a** Extracted maximum amplitude values without (undamaged, with indices i, white region) and with reversible damage D04 (indices j, gray region). **b** SD is calculated according to the two arrows (upper arrow: no damage detected so far; lower arrow: after damage detection). The decisive factor in the damaged case is the fixation of the last undamaged measurement ($A_{i=\text{end}}$) as the baseline. For examination purposes, we performed fixation manually

value decomposition, which differ in numerical performance, while singular value decomposition is advantageous.

In this paper, recurrence quantification analysis (RQA) is presented as a new approach to continuous baseline update and compared to the two selected established, non-interdependent signal features maximum amplitude (MaxSignal) and singular value decomposition (SVD) using datasets under varying temperatures with reversible damage (represented by an aluminum disc mounted on the surface of the specimen by tacky tape) at different positions [8].

2 Theoretical background

2.1 Continuous baseline update

The basic idea of the continuous baseline update approach is to compare an actual measurement at time t_1 with a former one at time t_0 (the so-called baseline) to separate temperature- and damage-induced signal changes. Extracted features from both the baseline and the actual signal are compared and evaluated. For this purpose, a wide variety of non-interdependent signal features can be used. One challenge of the continuous baseline update approach is to find and use the most suitable signal feature for damage detection. This paper investigates, as examples, three different features. The studied new approach of recurrence quantification analysis is further enhanced in Brandt et al. [9]. Figure 1 shows and explains the continuous baseline update approach exemplarily using the maximum amplitude value of the signals as an extracted feature.

The continuous baseline update approach assumes that damage causes higher signal changes than temperature changes do. If damage suddenly occurs, the signal change will exceed a defined threshold and indicate damage. If the threshold is not exceeded, the measurement at time t_1 will replace the signal at time t_0 and become the new baseline to compensate for the temperature effect. If damage is recognized, the baseline will be fixed and no longer be updated.

To subsequently define a threshold, the signal discrepancy [8]:

$$\mathrm{SD} = \left|\frac{F_\mathrm{a} - F_\mathrm{p}}{F_\mathrm{p}}\right| \cdot 100\%, \tag{1}$$

is introduced. Equation (1) calculates the difference between the feature of the previous (baseline) signal F_p (at t_0) and the one of the actual signal F_a (at t_1) and describes a percent change. If a threshold is exceeded, the calculation of SD changes according to the fixed baseline from that point on. In Eq. (1), F_p remains a constant value and F_a changes with a new measurement (see gray arrow in Fig. 1: $F_\mathrm{p} = A_{i=\text{end}} = \text{const}$). For the evaluation of the feature extraction methods, this paper introduces two different thresholds (see Fig. 3 for illustration):

$$Q = \frac{\mathrm{SD3}}{\mathrm{SD1}}, \tag{2}$$

$$R = \mathrm{SD3} - \mathrm{SD2}. \tag{3}$$

Here SD1, SD2, and SD3 are calculated according to Eq. (1) and denote characteristic signal discrepancy values with SD1: highest SD value in the region without damage; SD2: SD value of the last measurement before damage insertion; SD3: SD value of the first measurement after damage insertion. Q describes the ratio of the SD value of the first signal after damage insertion (SD3) and the highest undamaged one (SD1). R is the difference between the SD value of the first signal after damage insertion (SD3) and the last one before (SD2). Thus, Q is based on the SD ratio, while R uses changes of two subsequent SD values to detect damage. For application, the two thresholds differ in the need to store data. Q needs to check the maximal SD every time until damage insertion, while R only uses the SD of the previous measurement.

2.2 Recurrence quantification analysis

Recurrence quantification analysis (RQA), a tool of (nonlinear) time series analysis, has started with the invention of recurrence plots (RPs) in 1987 [10]. The motivation was to create a two-dimensional, visually accessible plot for high-dimensional nonlinear chaotic systems [11].

When applied to time series, the usual first step is to create a representation in a higher-dimensional space. The usual method of time delay embedding [12] is simple in implementation with delayed versions of the time series as additional dimensions, involving time delay τ and embedding dimension d (details and execution e.g. [13, 14]).

A recurrence matrix is generated from the multi-dimensional (embedded) time series through the following steps:

- Creation of a distance matrix

$$D_{i,j} = \|\mathrm{x}_i - \mathrm{x}_j\|, \tag{4}$$

having the size of the length n of the embedded time series to the square. The matrix thus contains the distances $\|\|$ (e.g. Euclidean distance) between every (embedded) time point x_i and x_j at the ith and jth position.

- Creation of a recurrence matrix (thresholded distance matrix)

$$R_{i,j} = \theta(\epsilon - D_{i,j}), \tag{5}$$

where the Heaviside-function θ maps positive values to one and negative values to zero. Thus, a pair of (time) points in space that are "near" to each other (nearer than a threshold ϵ) create a recurrence point in the matrix, with value one.

The visualization of the recurrence matrix as a black-and-white recurrence plot (RP) gives insights into dynamical systems, e.g., distinguishing between periodic, random, or chaotic systems [13] or detecting drifts [10]. A few years after its creation, recurrence quantification analysis (RQA) as the quantification of the information that is contained in an RP into several features emerged [15–17] (see [18] for a short historical review). The simplest feature is the recurrence rate RR, the ratio of recurrence points to all points of the plot:

$$\mathrm{RR} = \sum_{i,j}^{n} \frac{R_{i,j}}{n^2}, \tag{6}$$

which is used in this paper. (To be exact, the main diagonal of the recurrence plot, the line of identity, is not taken into account for the computations in this paper. The line of identity contains only a recurrence point because a point is always identical to itself, and thus also recurrent with itself.)

The determination of embedding parameters and the recurrence threshold ϵ can be chosen in several ways [17]. We apply a data-driven approach, cf. [14]: parameters are varied in a wide range, and the parameter set leading to optimum results (depending on the task) is chosen.

RQA has developed over the last 30 years from a method for research on chaotic systems to a versatile method of time series analysis; its use increases constantly [19] and is distributed over several disciplines [13, 20].

3 Results and discussion

3.1 Data processing

In the continuous baseline updating approach, complex feature extraction methods SVD [8] and RR of recurrence quantification analysis are compared to MaxSignal, using temperature-dependent GUW data from [8]. These three selected signal features are independent of each other.

Figure 2 a sketches the experimental setup. Six piezoelectric transducers (T1–T12) were each mounted on two opposite sides of a CFRP plate. The individual actuator-sensor pairs were measured in a round-robin test with the pitch-catch method with excitation signals of a 5-cycle Hann-filtered sine wave amplified to ± 100 V. Experiments were conducted by cyclically temperature variation in the range of 20–60 °C in 0.5 °C steps and relative humidity of 50%. At each temperature step and actuator-sensor path, the excitation frequency range was 40–260 kHz in 20 kHz steps. An aluminum disk mounted on the surface with tacky tape simulated damage (positions D04 and D24). Measurements were performed at two temperature cycles in the damage-free case and one in the damaged case with a 10 MHz sampling frequency and 13,108 data points for each signal.

For analyses, we apply continuous baseline updating to data sets from 0.3 to 1.3 ms (10,000 data points) at 40 kHz and temperature changes of 5 °C as depicted in Fig. 2a with reversible damage D04 and D24 in the actuator-sensor path T6–T12 (D04) and T1–T7 (D24). Compared to the scenario described in [8] with a temperature change of 0.5 °C between updated data sets, the temperature step of 5 °C in this work represents an enormous change and challenge to the continuous baseline updating approach and the different feature extraction methods. With this data selection, we use similar transducer paths to view the position dependence of damage. The challenge is to reliably distinguish between temperature- and damage-induced signal changes (Fig. 2b, c). At first glance, the reversible damage causes a significant amplitude attenuation of

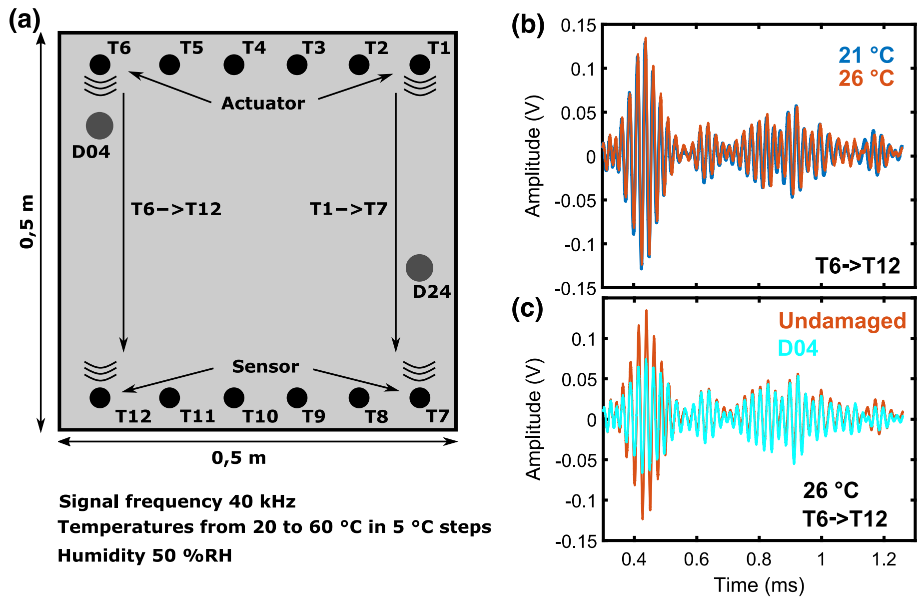

Fig. 2 **a** Schematic representation of the experimental conditions used. The actuator-sensor paths T6 to T12 and T1 to T7 are analyzed for the reversible damage D04 and D24, respectively. Effect of **b** temperature and **c** damage on wave propagation

the maxima amplitudes at 0.45 ms. Thus, it is reasonable to assume that feature extraction methods that depend on the global maximum are sensitive to damage insertions.

3.2 Analysis of the signal discrepancy data

Simple feature MaxSignal, as well as more complex features such as SVD and RR are used to calculate the SD in continuous baseline updating. For RR out of RQA, we have determined the parameters in a data-driven approach and a training/test manner: parameters are varied in a wide range; the parameters leading to the highest difference in RR values of ultrasonic signals determined at no defects on the one hand and defects, on the other hand, were chosen. The best parameters obtained at defect D04, transducer path T6 → T12, are used for computation of recurrence rates at defect D24 (transducer path T1 → T7), and vice versa (see Table 1).

Figure 3 illustrates an example of the SD profiles of MaxSignal, SVD, and RR. Damage D04 was introduced at a temperature change from 21 to 26 °C (a–c) and D24 from 51 to 46 °C (d–f). For D04, a clear, sharp separation between the undamaged (SD values below 5%) and the damaged case (SD values above 10%) characterizes the three methods. However, SD values differ hugely between methods, e.g., for MaxSignal, undamaged values are below 5%, and damaged ones are in the range of 30–50% in contrast to RR with up to 1% and 10–15%. The situation differs for D24; for example, the SD values of MaxSignal for signals without damage increase up to 10%, with defect SD values as low as 15% occur. For SVD and D24, the SD values of the last three signals are close to the highest of the undamaged ones. That indicates the limit of the method.

To compare the methods with each other quantitatively, the next step is to normalize. Q (Eq. 2) is already a normalized quantity. The maximal SD difference between adjacent measurements i and $(i-1)$ in the undamaged region (Fig. 1) normalizes R (Eq. 3) to:

$$R_{\mathrm{n}} = \frac{\mathrm{SD3} - \mathrm{SD2}}{\max|\mathrm{SD}_i - \mathrm{SD}_{i-1}|}. \tag{7}$$

When considering the distinction between signal changes caused by temperature effects and damage, there are two cases:

$$Q = \begin{cases} \leq 1; \text{damage indistinguishably from temperature effect} \\ \text{else; damage distinguishably from temperature effect} \end{cases}, \tag{8}$$

$$R_{\mathrm{n}} = \begin{cases} \leq 1; \text{damage indistinguishably from temperature effect} \\ \text{else; damage distinguishably from temperature effect} \end{cases}. \tag{9}$$

Table 1 RQA parameters

Parameter	Used for evaluation of signals of D4, T6 → T12 Determined on D24, T1 → T7	Used for evaluation of signals of D24, T1 → T7 Determined on D4, T6 → T12
Embedding dimension d	2	3
Delay τ	70	90
Recurrence threshold ϵ	0.1	0.1

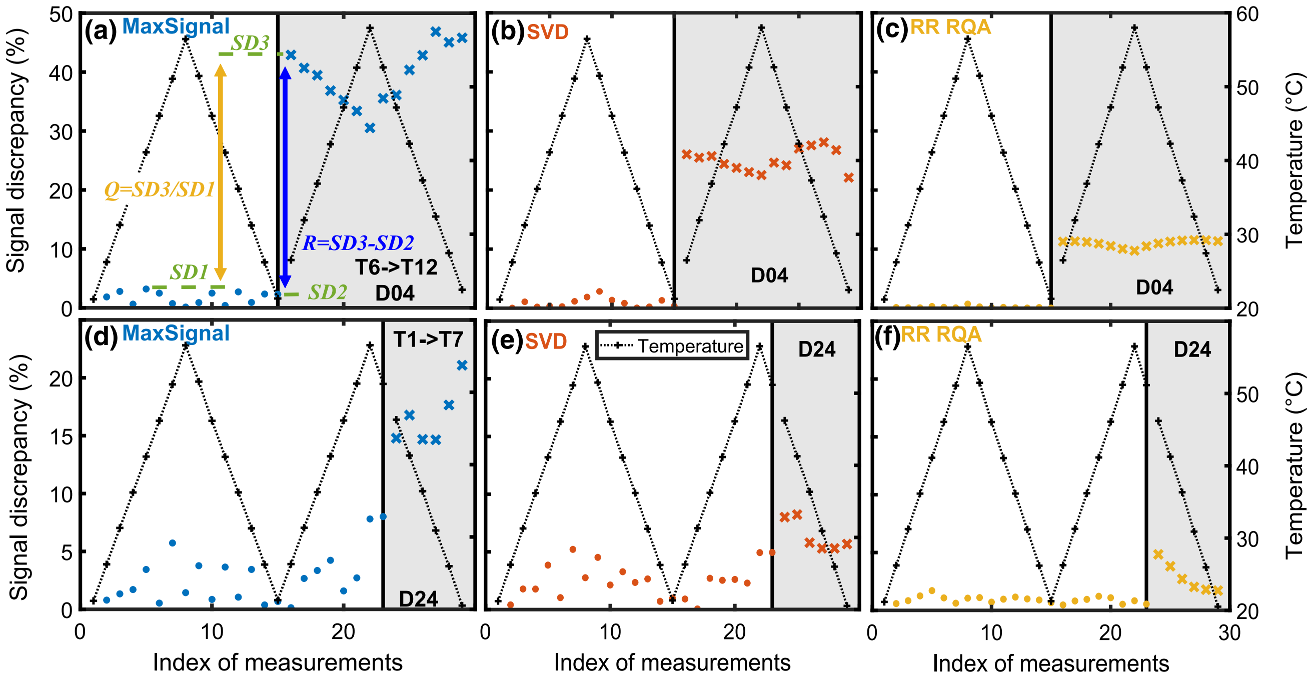

Fig. 3 Quantification of methods MaxSignal (**a**, **d**), SVD (**b**, **e**), and RR RQA (**c**, **f**) by introducing Q and R (Eqs. 2 and 3). **a**–**c** Depict the curves for the insertion D04 at 26 °C ascending and **d**–**f** show D24 at 46 °C descending temperature. R describes the absolute change in signal discrepancy at the transition from undamaged to damaged. Q characterizes the ratio between the maximum SD before and the first SD after damage insertion

If an SD value (Q) or difference (R_n) of the damaged data is at most as large as the maximum of the undamaged set, the damage cannot be distinguished and detected in the continuous baseline update approach.

Figure 4 plots the Q and R_n values for D04 and D24. Additionally drawn as the area marked in gray and white are the distinctions. On the one hand, the values of Q and R_n for all three methods for D04 (Fig. 4a, c) are noticeably higher than for D24 (Fig. 4b, d). On the other hand, SVD and MaxSignal provide comparable results, while RR outperforms Q for D04 and R_n for D24 (Fig. 4a, d). At D24 and 51–46 °C, the R_n values of SVD and MaxSignal are even on the border of indistinguishability. The RR has, in contrast, the value 7. The position dependence of the reversible damage can explain the differences between D04 and D24 with similar actuator-sensor paths. While D04 is close to the actuator, D24 is close to the sensor. The reversible damage causes attenuation of the multimode GUWs. Since the amplitude attenuation is proportional to the square root of the propagation distance, an enlarged distance between damage and sensor results in higher signal deviations and the observable differences between D04 and D24. The strong amplitude attenuation in Fig. 2b and Q and R_n values for MaxSignal based on amplitude attenuation support the explanation. Similar results from MaxSignal and SVD also support the assumption of amplitude attenuation as the main signal change since SVD calculates one characterizing value per sensor signal, i.e., the dominant signal change factors reflected in the singular value. MaxSignal is limited to damage classes characterized by maximum amplitude changes. On the other hand, SVD also includes changes in signal shape, e.g., due to interaction with scattered partial waves. The performance of recurrence quantification analysis with the feature recurrence rate is connected to the signal height as well, as recurrence rates go up for signals with smaller amplitude measured at the damage. RQA however apparently picks up the effects in a more comprehensive way than the two simpler features MaxSignal and SVD. The better performance of RQA results from a higher sensitivity of RR to lower signal changes than SVD. An explanation may be the determination of parameters in a data-driven approach and a training manner using similar actor-sensor pairs.

A further RQA-based approach to this application can be found in [9], including more details on the process of training, i.e., parameter determination, which is in principle equal to the one described here.

4 Conclusion

The separation of temperature- and damage-induced signal changes was investigated within the continuous baseline update approach using publicly available guided ultrasonic wave data with reversible damage and varying temperatures. Recurrence quantification analysis, singular value decomposition, and maximum amplitude were used for feature extraction. For quantitative

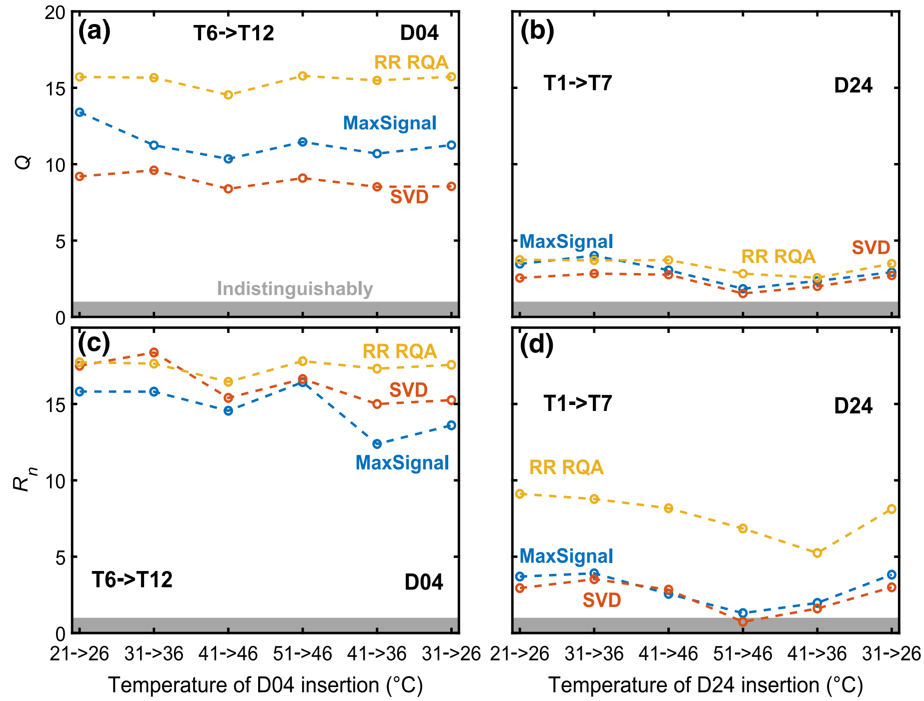

Fig. 4 Method comparison for damage detection of D04 (**a**, **c**) and D24 (**b**, **d**): using Q (Eq. 2) (**a**, **b**) and R_n (Eq. 7) (**c**, **d**). For $Q \leq 1$ or $R_n \leq 1$, respectively, a method cannot distinguish between the undamaged and damaged case (gray area) due to the temperature-induced feature changes

comparison of the different approaches, two parameters, based on the change in signal discrepancy, were introduced. Damage at two different positions causes signal attenuation. Damage detection is better for the damage placed closer to the actuator. The feature extraction methods maximum amplitude and singular value decomposition provided comparable results. The recurrence rate allowed for better damage detection: it provided reliable results even under challenging conditions to detect damage. We showed that continuous baseline works on simple plate structures for relatively high-temperature steps of 5 °C.

Acknowledgements The work of Faserinstitut Bremen e. V. was financially supported by the Federal Ministry for Economic Affairs and Climate Action based on a decision by the German Bundestag under Grant numbers 49VF180016 and ZF4554305LP9.

Funding Information Open Access funding enabled and organized by Projekt DEAL.

Data Availability Statement The datasets analyzed during the current study are available in the repository https://doi.org/10.6084/m9.figshare.c.4488089.v1. From the available data sets "OGW_CFRP_Temperature_udam", "OGW_CFRP_Temperature_dam_D04", and "OGW_CFRP_Temperature_dam_D24" were used.

Declarations

Conflict of interest The authors declare that they have no financial and personal relationships with other people or organizations that could inappropriately influence this work.

References

1. J.E. Michaels, Struct. Health Monit. (SHM) Aerosp. Struct. 255–284 (2016). https://doi.org/10.1016/B978-0-08-100148-6.00009-3
2. R. Gorgin, Y. Luo, Z. Wu, Ultrasonics (2020). https://doi.org/10.1016/j.ultras.2020.106114
3. S.B. Kim, H. Sohn, Smart Mater. Struct. **16**, 6 (2007). https://doi.org/10.1088/0964-1726/16/6/042
4. S.R. Anton, D.J. Inman, G. Park, AIAA J. **47**, 8 (2009). https://doi.org/10.2514/1.43252
5. J.-S. Lee, G. Park, C.-G. Kim et al., J. Intell. Mater. Syst. Struct. **22**, 2 (2011). https://doi.org/10.1177/1045389X10395643

6. O. Putkis, A.J. Croxford, Smart Mater. Struct. **22**, 5 (2013). https://doi.org/10.1088/0964-1726/22/5/055029
7. G.D. Connolly, J. Li, S.I. Rokhlin, NDT & E Int. (2013). https://doi.org/10.1016/j.ndteint.2013.01.009
8. J. Moll, C. Kexel, S. Pötzsch et al., Sci. Data **6**, 1 (2019). https://doi.org/10.1038/s41597-019-0208-1
9. C. Brandt, N. Marwan, Eur. Phys. J. Spec. Top. (2022). https://doi.org/10.1140/epjs/s11734-022-00701-8
10. J.-P. Eckmann, S.O. Kamphorst, D. Ruelle, Europhys. Lett. **4**, 9 (1987). https://doi.org/10.1209/0295-5075/4/9/004
11. S. Oliffson Kamphorst, 7th International Symposium on Recurrence Plots (Sao Paulo, 2017). Keynote Lecture: The Very Beginning of Recurrence Plots. http://symposium.recurrence-plot.tk/programme2017.pdf
12. F. Takens, in *Lecture Notes in Mathematics*. ed. by D. Rand, L.-S. Young (Springer, Berlin, 1981), pp.366–381
13. N. Marwan, C.M. Romano, M. Thiel et al., Phys. Rep. **438**, 5–6 (2007). https://doi.org/10.1016/j.physrep.2006.11.001
14. C. Brandt, in *Springer Proceedings in Physics*. ed. by C.L. Webber, C. Ioana, N. Marwan (Springer International Publishing, Cham, 2016), pp.355–377
15. J.P. Zbilut, C.L. Webber, Phys. Lett. A **171**, 3–4 (1992). https://doi.org/10.1016/0375-9601(92)90426-M
16. C.L. Webber, J.P. Zbilut, J. Appl. Physiol. (1985) **76**, 2 (1994). https://doi.org/10.1152/jappl.1994.76.2.965
17. C.L. Webber, N. Marwan, *Recurrence Quantification Analysis* (Springer International Publishing, Cham, 2015)
18. C. Brandt, *Recurrence Quantification Compared to Fourier Analysis for Ultrasonic Non-destructive Testing of Carbon Fibre Reinforced Polymers* (Universität Bremen, Bremen, 2020)
19. N. Marwan, A Comprehensive Bibliography About RPs, RQA and Their Applications. http://www.recurrence-plot.tk/bibliography.php. Accessed 10 Sept 2021.
20. C.L. Webber, C. Ioana, N. Marwan, *Recurrence Plots and Their Quantifications: Expanding Horizons* (Springer International Publishing, Cham, 2016)